

# **“Detection of linear ego-acceleration during 3D-shape perception”**

**Bachelorarbeit  
der Mathematisch-Naturwissenschaftlichen Fakultät  
der Eberhard Karls Universität Tübingen**

**vorgelegt von**

**Florian Ott**

**Tübingen, August 2013**

## **Erklärung:**

Hiermit erkläre ich,

- dass ich diese Arbeit selbst verfasst und keine anderen als die angegebenen Quellen und Hilfsmittel benutzt habe.
- dass die eingereichte Arbeit weder vollständig noch in wesentlichen Teilen Gegenstand eines anderen Prüfungsverfahrens gewesen ist.

Tübingen, den 28. August 2013

# Table of Contents

Abstract / Zusammenfassung.....	4
1 Introduction.....	6
1.1 Egomotion from optic flow .....	6
1.2 Ego-acceleration from optic flow .....	7
1.3 Ego-acceleration in a three-dimensional Environment.....	7
1.4 Aim of this Study .....	8
2 Methods .....	9
2.1 Creating the Model.....	9
2.2 Rendering Software.....	10
2.3 Stimuli.....	10
2.4 Stereoscope.....	11
2.5 Procedure .....	12
2.6 Participants.....	12
2.7 Data Analysis .....	13
3 Results .....	15
4 Discussion .....	18
4.1 Interpretation of the Results .....	18
4.2 Implications for Cue integration.....	18
4.3 Comparability to previous findings .....	19
4.4 Future prospects .....	20

# List of Figures

Figure 2.1 3D Models of the block corridors .....	9
Figure 2.2 Stimuli .....	11
Figure 2.3 Stereoscope setup .....	12
Figure 3.1 Results of each subject.....	15
Figure 3.2 Results for all subjects.....	16
Figure 4.1 Random dot stimulus for comparisons .....	19

## Zusammenfassung

Die Intention dieser Arbeit war, zu untersuchen wie der Mensch seine Eigenebeschleunigung, bei gleichzeitiger Wahrnehmung von dreidimensionalen Objekten, einschätzen kann. Es ist bekannt, dass der optische Fluss ausgenutzt werden kann, um verschiedene Parameter der Eigenbewegung zu erfassen. So sind zum Beispiel die Wahrnehmung von Rotationen, Bewegungsrichtung und die Zeit bis zur Kollision mit einem Gegenstand (time-to-contact) auf Stimulationen via optischen Fluss zurückzuführen. Kürzlich konnte gezeigt werden, dass auch die Wahrnehmung von Eigenbeschleunigung vom optischen Fluss abhängt. Die Annahme der aktuellen Studie ist jedoch, dass Einschätzung der Eigenbeschleunigung, in einer realistischen Umgebung, nicht nur vom optischen Fluss abhängt, sondern auch vom Tiefenprofil der Umgebung. Theoretisch kann gezeigt werden, dass diese zwei Faktoren, Eigenbeschleunigung und Tiefenprofil auseinander gehalten werden können, was ein korrektes Einschätzen der Eigenbeschleunigung prinzipiell möglich macht. Dies führte zur Hypothese, dass der Menschen fähig ist seine Eigenbeschleunigung, während eines simulierten Fluges durch einen Korridor, korrekt einzuschätzen, obwohl dieser Korridor seine Form verändert.

Um die Hypothese zu testen wurde ein psychophysisches Experiment durchgeführt, in dem die Teilnehmer entscheiden mussten, ob sie während des Fluges durch den Korridor beschleunigt oder abgebremst worden sind. Dabei wurden zwölf verschiedenen Beschleunigungsraten eingesetzt, darunter sehr deutliche und sehr kleine Beschleunigungen. Der Korridor bestand aus zwei Reihen mit massiven, farbigen Blöcken. Der Korridor war entweder gerade, verengend oder erweiternd. Um den Eindruck der Räumlichkeit zu verstärken, wurden die Stimuli durch ein Stereoskop gezeigt. Aus den gemessenen Daten wurden psychometrische Funktionen angenähert.

Die Ergebnisse dieser Arbeit zeigten eine signifikante Verschiebung der psychometrischen Kurven des verengenden und des erweiternden Korridors. Dies zeigte, dass die Teilnehmer ihre Eigenbeschleunigung im verengenden Korridor überschätzen und im erweiternden Korridor unterschätzen. Die aufgestellte Hypothese musste, zumindest teilweise, zurückgewiesen werden. Es scheint als sei der Grad der Verwechslung von Eigenbeschleunigung und Geometrie der Umgebung gering, im Vergleich zu vorangegangenen Experimenten von Festl et al. (2012) und Becker (2013). Ein direkter Vergleich mit diesen Experimenten ist jedoch auf Grund von Unterschieden im Stimulus kritisch zu betrachten.

Nichtsdestotrotz, es konnte gezeigt werden, dass optischer Fluss, sogar in einer relativ realistischen Umgebung mit drei-dimensionalen Objekten, eine wichtige Rolle bei der Einschätzung von Eigenbeschleunigung spielt. Es scheint jedoch wahrscheinlich dass die Erfassung des Tiefenprofils der Umgebung die Eigenbeschleunigungs-Wahrnehmung beeinflusst. Ein Mechanismus bei dem die aktuelle Geschwindigkeit mit einer internen Vorstellung der Objekt-Beobachter Distanz skaliert wird, könnte die Eigenbeschleunigungswahrnehmung verbessern. Die Frage wie die Verarbeitung von optischem Fluss mit der Wahrnehmung von Tiefe interagiert bedarf jedoch weiterer Untersuchung.

## Abstract

The intention of this work was to investigate the human ability to estimate ego-acceleration during the perception of three dimensional objects. It has long been known that optic flow plays an important role in the estimation of various egomotion parameters such as rotation, direction or time to contact. And recently it has been shown that ego-acceleration perception also relies on optic flow. The underlying assumption of the current study was that in a realistic environment, ego-acceleration estimates do not only depend on optic flow, but also on the depth profile of the surroundings. Theoretically, it can be shown that these two factors, ego-acceleration and environment shape, can be separated, allowing a correct judgment of ego-acceleration. This led to the hypothesis that human observers might be able to correctly estimate ego-acceleration during a flight through a corridor, although this corridor alters in shape.

To test the hypothesis, the participants had to decide whether they had been accelerated or decelerated during a simulated “flight” through a corridor. Twelve different acceleration rates were applied, including both obvious and more subtle accelerations and decelerations. The corridor consisted of two arrays of colored, solid blocks and appeared in three different shapes: straight, narrowing and widening. The simulations were viewed through a stereoscope. Psychometric functions were fitted for each corridor condition.

The results of the current study showed a significant shift between the psychometric function for the narrowing and the widening corridor, which means that participants overestimated ego-acceleration in the narrowing corridor and underestimated ego-acceleration in the widening corridor. Therefore, the initial hypothesis had, at least partially to be rejected. It seems that the confusion of scene geometry and actual ego-acceleration is relatively small, compared to precursory experiments of Festl et al. (2012) and Becker (2013). However, differences in the stimuli render direct comparisons difficult. Nevertheless the current study could provide evidence that even in an environment with distinct three-dimensional objects, optic flow is still an important source for ego-acceleration perception. A mechanism is proposed that the actual ego-velocity could be scaled by an internal perception of observer-object distance. However, the question of how the processing of optic flow interacts with the perception of depth remains to be answered.

# 1 Introduction

## 1.1 Egomotion from optic flow

Visual perception plays an important role for the control of egomotion in the human being. Other stimulation, including proprioceptive, vestibular, auditory and haptic, provides useful information of the current state of locomotion, but in the absence of light one is no longer able to navigate confidently through the environment. The visual detection of motion and the visual perception of egomotion are basic requirements for the survival in nature. Therefore an analysis must include the ecological affordances of those abilities. From the light that reaches the eye, information has to be extracted, sufficient to complete biologically important tasks, such as reaching a goal (e.g. food), escaping from predators, catching prey or avoiding collision with obstacles. Due to its biological importance, an own “sense” has evolved to visually access self-motion. The basic stimulation that feeds this “sense” can be described as the optic flow (Gibson, 1958).

The optic flow is defined as the pattern of retinal activity during movement through a static environment (Gibson, 1950). Solid matter of the physical world reflects light in all directions. One light beam from each point of the visual field is projected onto the retina, forming an image of the environment. When travelling through the world, the single features of the image are shifted in the visual field and therefore a specific array of retinal receptors is stimulated. The optic flow is sometimes also called retinal flow. The retinal projection of the movement of one point in the scene can be described as a two-dimensional motion vector. A motion vector gives information about the direction and the velocity of the movement. The direction of the flow vector depends upon the direction of the observer’s movement. When the observer moves to the right, the motion vector aims to the left side. When the observer travels straight ahead, all motion vectors emanate radially from the direction of the observer’s movement. This point can also be called the focus of expansion (FOE). The velocity of the flow vector depends not only on the actual speed of the observer, but also on the distance between the observer and the passing element of the scenery. Points that are nearby to the observer are moving faster than points that are further away. The velocity of the flow vector in the focus of expansion is zero. The speed difference between two points in the same visual angle, but with different distances, is called motion parallax. In reality optic flow often arises not solely from pure translational or horizontal movement. Due to head and eye movements or one’s own curved trajectory, a rotatory component is added to optic flow. One retinal flow vector  $\vec{v}$  of an image point  $p$  can mathematically be described as a function of the translation  $T$ , the rotation  $\Omega$  of the eye and the distance  $Z$  from the point to the eye:

$$\vec{v} = f(T, \Omega, Z). \quad (1)$$

Distance and translation are coupled so that the flow depends on the quotient  $T/Z$  (Longuet-Higgins and Prazdny, 1980).

Experimental research has shown that optic flow is exploited to control many behavioral tasks. Evidence that people make use of the optic flow to steer towards a goal has been provided by Warren et al. (2001). In contrast to the hypothesis that the observer walks into the direction of the perceived angle of the object, the study has shown that the observer adjusts the FOE, which is immanent to the optic flow,

onto the target. This strategy is robust with respect to involuntary shifts of heading. Avoiding obstacles during locomotion is another biologically important task. It has been shown that humans can estimate the time, until they reach an approaching object with constant velocity using optic flow. This parameter is often termed time to contact (TTC) or time to passage (TTP) (e. g. Kaiser and Hecht, 1995). Furthermore optic flow signals are used to maintain an upright body posture. When subjects are being exposed to a periodically expanding and contracting large-scale optic flow stimulus, the body of the subjects begins to sway forth and back in the same periodicity as the stimulus contracts and expands. This effect was especially observed in very young children (Lee and Aronson, 1974).

## **1.2 Ego-acceleration from optic flow**

Theoretically, translational velocity cannot be recovered from optic flow, because the velocity of one flow vector depends on both, the velocity of the observer and the distance between the observer and object. Ego-velocity could only be calibrated with an independent measurement of distance (Frenz and Lappe, 2005). In contrast ego-acceleration could theoretically be estimated from optic flow (feature based approach). The essential variable is the ratio of the acceleration and the velocity, which is independent from the scene geometry (Festl et al., 2012). Contradictory to this hypothesis, experimental analysis showed that the human observer does not make use of those acceleration cues. During a simulated flight through a narrowing corridor, the participants failed to disentangle depth information from the actual acceleration, resulting in an overestimation of acceleration (Festl et al., 2012). This study gives weight to a different mechanism of ego-acceleration estimation. The matched filter approach is based on the assumption that all local motion vectors are matched to an expected flow field (for a given egomotion) and the matches are summed up for the estimation of ego-acceleration. Therefore the observer only uses retinal accelerations and neglects depth information during presentation of a pure optic flow stimulus. For a mathematical description of the two mentioned approaches concerning ego-acceleration estimation, see Festl et al. (2012).

## **1.3 Ego-acceleration in a three-dimensional Environment**

In a natural environment several visual cues are integrated by the observer to achieve an accurate perception of egomotion (for general information concerning cue integration see: Bühlhoff and Mallot, 1988; Ernst and Bühlhoff 2004). Ego-acceleration estimates are not only based on the processing of optic flow, but also on mechanisms which provide information on the geometry of the scene. Becker (2013) has shown that adding stereoscopic depth to an optic flow stimulus improves the perception of ego-acceleration, suggesting that the processing of optic flow and stereoscopic depth interact in a cooperative manner.

These findings are consistent with the concept of velocity constancy (Distler et al., 2000). Objects moving with the same physical velocity, but with different distances to the observer have different angular velocities on the retina. Yet the human observer is able to correctly judge the physical speed of the object although the retinal velocity is different. It is suggested that the observer scales retinal velocity relative to an inner perception of observer-object distance. The better the perception of this inner-distance is, the better the estimate of the physical velocity will be. Distler et al. (2000) investigated how different depth cues contribute to velocity constancy. The cues were perspective size, texture of the ground plane, observer viewing height, disparity and motion parallax. When all of these cues were

available, almost perfect velocity constancy could be obtained. When several cues were omitted, estimates of the physical velocity lost accuracy. It should be stated that the cues did not interact in a linear fashion. The combination of different cues is more than the mere sum of its elements.

#### **1.4 Aim of this Study**

The current investigation can be seen as a further element of a series of studies concerning the estimation of ego-acceleration. And this series of studies, in turn, can be interpreted as a reductionistic approach to understanding the processing of visual information, which underlies ego-acceleration detection. The first study of Festl et al. (2012) started with an experiment where only very basic visual information (optic flow) was presented to the observer. In subsequent experiments of Becker (2013) additional information, in the form of stereoscopic depth, was added to the stimulus. The current investigation sticks to the idea of its predecessors and consequently uses a more realistic environment with distinct 3D-objects.

Distler et al. (2000) addressed the question how visual cues are integrated in speed judgments of moving objects and came to the conclusion that observers integrate multiple depth cues to obtain velocity constancy. It is assumed that the phenomenon of velocity constancy can be transferred from object motion to an ego-motion context (henceforth called ego-velocity constancy). In the study of Festl et al. (2012), participants completely confused ego-acceleration and the scene geometry, due to a lack of spatial information. In Becker (2013) the performance of the participants was improved. Despite the availability of stereoscopic depth, however, the scene geometry and ego-acceleration could still not be completely disentangled. In the present study the participants had to estimate ego-acceleration during a simulated flight through a corridor which was alternating in shape (straight, narrowing, and widening). The corridor consists of two rows of solid blocks with shading and the stimulus was presented through a stereoscope. The set of cues offered, extended from retinal feature based flow (Festl et al., 2012) and feature-based flow in depth (Becker, 2013) to object motion (ego-velocity constancy) in 3D (see Distler et al., 2000). This stimulus should enable the observer to separate between scene geometry and ego-acceleration. The hypothesis of the present study therefore was that the subjects are able to correctly estimate their ego-acceleration both in a narrowing and in a widening corridor.



## 2 Methods

### 2.1 Creating the Model

The (block) corridor models were created with Multigen Creator (version 2.5.1) developed by Multigen-Paradigm (now Presagis). The Creator is a 3D modeling software which allows the user to generate precise and detailed virtual objects and environments. The created corridor models were saved in OpenFlight (.flt) a widely used format for real-time 3D-visualization.

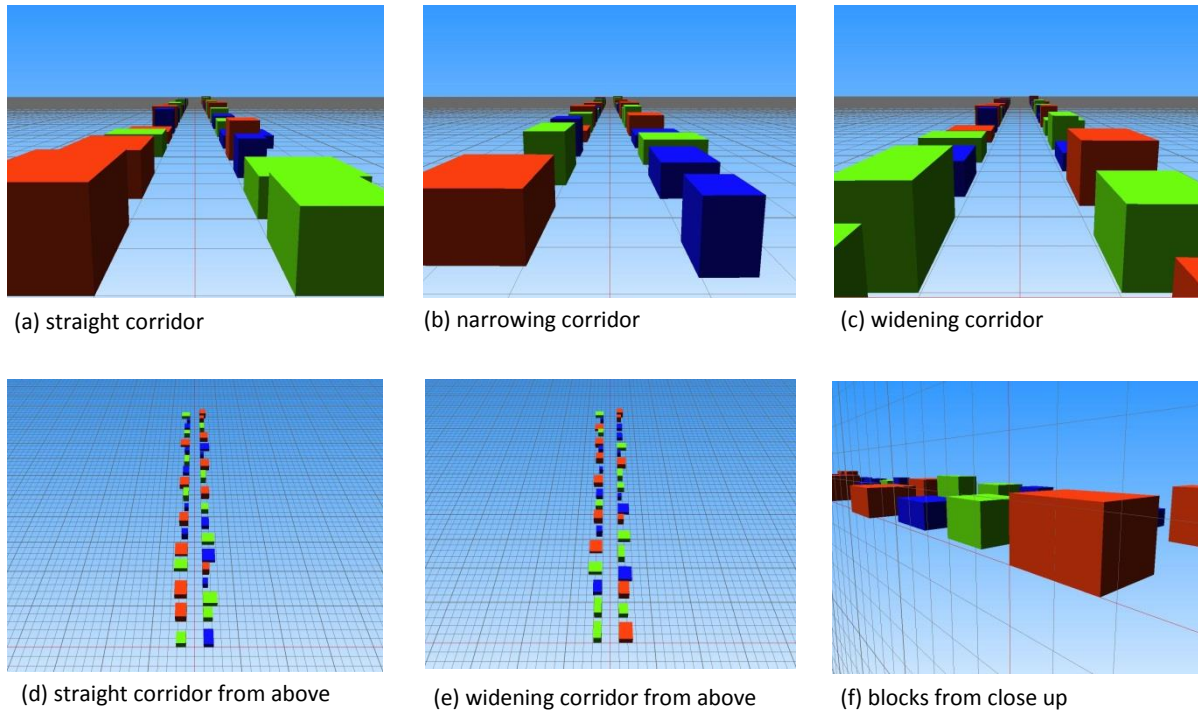


Figure 2.1. 3D-models of the corridors from different perspectives. The distance between two gridlines is one meter. Narrowing and widening corridors had an apical angle of one degree ( $0.5^\circ$  declines per side). The opening of the corridor had a width of two meters.

The model consisted of a corridor with solid-colored blocks on either side (Figure 2.1). The height of the blocks varied within a range from 0.4 to 1.1 meters, and the edges along the x and y-axes from 0.7 to 2 meters. The blocks had three different colors: red, green and blue. Eighteen blocks, differing in size and color, were aligned to each side of the corridor. The corridor as a whole had a length of 50 meters. Shading was added to the scene to strengthen the appearance of three-dimensionality. The corridor itself appeared in three conditions: straight, narrowing and widening. The straight corridor had parallel borders with a constant width of 2 meters. The narrowing corridor started with a width of 2 meters and then narrowed down to 1.5 meters at a distance of 30 meters, corresponding to an apical angle of 1 degree. The widening corridor started with a width of 2 meters and broadened to 2.5 meters at a distance of 30 meters, due to an apical angle of 1 degree. For the latter two cases, the blocks were congruently aligned to the trapezoidal form of the street. The interspace between two blocks on one side of the corridor varied within a range from 1 to 2 meters. To prevent participants from associating the corridor shape with the sequence of the houses, ten versions with alternated sequences of houses were designed for each corridor condition.

## 2.2 Rendering Software

To realize a virtual drive through the corridor on a stereoscopic setup, scenes were rendered with a software developed by Hannig (2012) and edited by Becker (2013). The program was written in C++. OpenSceneGraph (version 3.0.1), an open source 3D graphics toolkit, was used for the visual simulations. Microsoft Visual Studio 2008 (version 9.0.21022.8) was chosen as the development environment. For a detailed description of the program's classes, see Becker (2013).

The main difference between the prior and the present versions of the program is that distinct objects instead of only isolated dots were presented to the observer. Beyond that the number of models to be loaded increased from three to thirty. For this reason the "BuildScene" class, which takes care of loading the scenes to the scene tree, had to be adapted. Additional osg::Switch objects were added to enable switching between the scenes, while running the experiment. Additionally the class "Experiment" was changed. This class generated an array of randomly ordered "Trial" objects containing the relevant attributes for executing each single trial. "Trial" objects stored the index of a trial, the index of the loaded model, acceleration rates in  $m/s^2$  and  $m/frame^2$ , initial velocities and the answer of the subject for the actual trial. In the current program, the cycles of the for-loop, which add the model indices, were increased from three to thirty. This allowed the "Stereoscope" class, which contained the main executable function, to switch between the different models. Model 1-10 are straight corridors; 11-20 are narrowing corridors and 21-30 widening corridors.

## 2.3 Stimuli

The motion sequences were established by driving a virtual camera through the model scene. This sequence should simulate an ego-perspective "flight" through the corridor. The height of the camera was 0.5 meters and the view angle was centered in the corridor. The apical angle of the camera, and thereby the field of view, was  $112^\circ$  in horizontal direction and  $89^\circ$  in vertical direction. (Figure 2.2). Each sequence lasted 3 seconds (180 frames). As in the studies by Festl et al. (2012) and Becker (2013) twelve different levels of acceleration were used, ranging from  $-5.5 m/s^2$  to  $5.5 m/s^2$  in steps of  $1 m/s^2$ . The traveled distance was held constant at 30 meters, resulting in a constant mean velocity of  $v_m = 10 m/s$ , but with different initial velocities. Given both

$$v(t) = v_0 + at \text{ and } s(t) = v_0t + \frac{1}{2}at^2. \quad (2)$$

The initial velocity can be calculated

$$\begin{aligned} v_m &= \frac{s(t) - s(0)}{t} \\ &= \frac{v_0t + \frac{1}{2}at^2}{t} \\ &= v_0 + \frac{1}{2}at \\ v_0 &= v_m - \frac{1}{2}at. \end{aligned} \quad (3)$$

Since the experiment was run on a 60 Hertz monitor, velocities had to be divided by 60 and accelerations by 3600 to convert the units into  $m/frame$  and  $m/frame^2$ . Furthermore, a grey rectangle has been added to the scene, traveling with the subject and covering the end of the corridor. In general, humans have a conception of how parallel lines are converging in the distance. The cover should avoid that the participants draw conclusions from a linear perspective on the shape of the corridor.

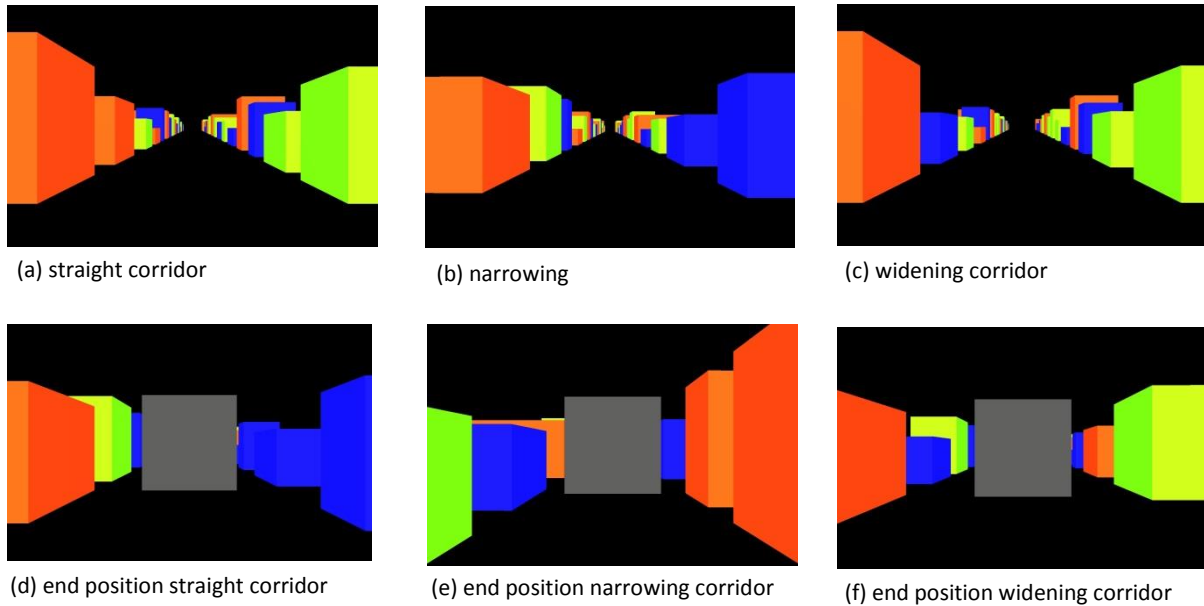
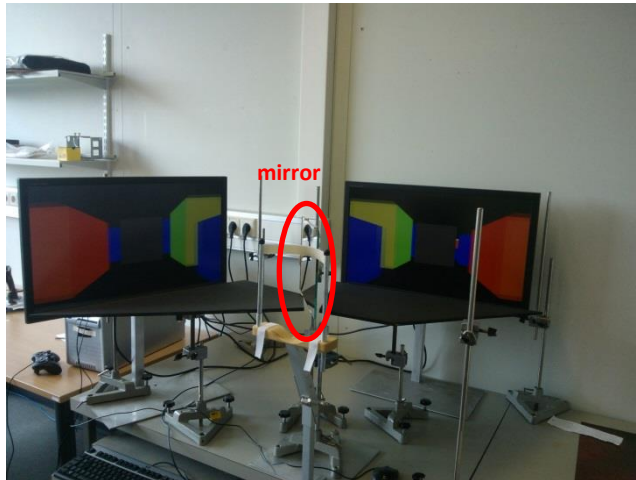


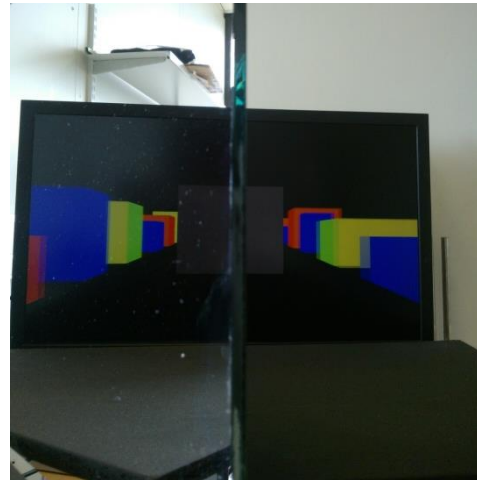
Figure 2.2. Snapshots taken during a running trial. Picture (a) – (c) show an ego-perspective view on the three different corridor shapes at the beginning of a trial. Picture (d) – (f) show what the subject sees at the end of a trial. In all simulations a grey cover was added to the scene, so that the participants could not see the end of the corridor.

## 2.4 Stereoscope

When one observes distant scenery, differences in perspective of objects far away become evanescent and thus, no stereoscopic depth is perceived. When objects are closer to the observer, the eyes converge, so that the optical axes intersect at the point of fixation. Now, different pictures of the object are projected on the two retinas. Due to the angle of the optic axes causing a horizontal disparity, the object reveals differences of perspective to each of the eyes. The three-dimensionality of an object, which the brain perceives, is constructed by the means of those disparate pictures. This is what is known as stereopsis (Wheatstone, 1838). The basic principle that enables a stereoscope to create an artificially induced impression of stereoscopic depth is that identical images are depicted on the retinas by objects of three dimensions and by their projection on the image planes. Therefore, it does not matter if two pictures of a two-dimensional projection of an object are shown separately to both eyes or if the object itself is regarded binocularly. Both practices will generate the same retinal stimulus and hence affect the same perception.



(a) Setup of the stereoscope (one mirror setup)



(b) View from the observer

Figure 2.3. Stereoscopic Setup. (a) A chin rest is placed in front of the mirror. From this position the participants looked straight at a plane mirror. The right eye receives the (non-mirrored) image of the right monitor and the left eye sees the mirrored image of the left monitor. During the running experiment the stereoscope was covered by a wooden plate. Dividing elements, made out of cotton, separated the light paths to avoid disturbing light reflections (not depicted in the figure). (b) Photograph taken from the position of the observer. The left half of the picture shows the reflected image of the left monitor and the other half shows the picture of the right monitor. The brain fuses the two pictures into one stereo impression.

In the current study the stimuli were presented by a stereoscope to provide a vivid impression of three-dimensionality. The stereoscope used was a modified version of the 1838 invented Wheatstone-Stereoscope (Wheatstone, 1838; Kollin and Hollander, 2007). The setup included a plane mirror in front of the face of the observer and two 27'' monitors (Figure 2.3). If the subject is seated right in front of the apparatus, the left eye only sees the left monitor and the right eye only sees the right monitor. To allow the participants to fuse the two pictures into one stereo impression, a perspective projection had to be applied to the stereo-halves. To create the pairs of stereo view, a pre-assembled method from the OpenSceneGraph-library was used.

The stereoscope was set up by Till Becker as in previous experiments on motion estimation. For additional details on construction and validating of the stereoscope see Becker (2013).

## 2.5 Procedure

Motion sequences had been individually shown to the participants. In a psychophysical task, according to the method of constant stimuli, the subjects had to evaluate whether they had been accelerated or decelerated (Yes-No-Paradigm). The choice was made after each trial by clicking on the left mouse button for deceleration or by clicking on the right button for acceleration. Each model (ten per corridor shape) was randomly loaded and acceleration conditions were randomly allocated. This should prevent habituation effects and the ability of the subjects to predict the next acceleration condition. In total 720 trials had to be completed by the subject, i.e., twenty repetitions for each acceleration rate and corridor shape (20x12x3). All together the experiment took between 40 and 60 minutes.

## 2.6 Participants

Seven volunteers participated in this experiment (six male and one female, aged 20 to 28). MG, FH and DF were complete naïve about the purpose of the experiment. DV, IG and SK had prior knowledge,

because they had attended a presentation on the topic of this study. All participants had normal or were corrected to normal vision.

## 2.7 Data Analysis

Data analysis was performed using Matlab (version R2013a) with the psychophysics toolbox, “Palamedes” (version 1.6.0).

The raw data was saved in the form of a table containing the characteristics of each trial (Table 2.1). The table consisted of seven columns including corridor shape, session number (irrelevant), trial-count, trial number (out of 720), acceleration-rate, yes-no answer (1 = yes, -1 = no) and the number of the loaded model (1-30). Before further data analysis could be conducted, the data had to be preprocessed. For each corridor shape and each acceleration-rate, the number of answers “acceleration, yes” had to be determined.

Shape	Session	Trial count	Trial number	Acceleration	Answer	Model number
3	1	1	349	-5.5	-1	30
1	1	2	7	0.5	1	1
2	1	3	153	2.5	1	13
...	...	...	...	...	...	...

Table 2.1. Example of a raw data file after three trials of the experiment.

Psychometric functions were fitted to the data. The psychometric data was modeled using a logistic function given as:

$$F_L(x; \alpha; \beta) = \frac{1}{1 + \exp(-\beta(x - \alpha))} \quad (4)$$

Alpha is the threshold characterizing the turning point of the sigmoidal function and beta describes the slope of the curve. The toolbox function, PAL\_PFML\_Fit, determined the two parameters using a maximum likelihood criterion. The computer iteratively searched through a range of possible values for alpha and beta and found those parameters that generated the curve which matched best the experimental data. Whereas threshold and slope describe the properties of the underlying sensory mechanisms, another two parameters could be set to determine the psychometric function: the guess rate  $\gamma$  and the lapse rate  $\lambda$ . Gamma is the probability to give the right answer, although the sensory system has not detected the stimulus, and lambda is the probability to give a wrong answer, despite sufficiently high stimulus intensity. Both gamma and lambda were set at a fixed value of zero.

Due to a limited number of trials per acceleration-rate, the estimated  $\alpha$  and  $\beta$  will always differ from the “true” values. “Palamedes” offered a method to evaluate how well the calculated parameters approximated the “true” parameters. The toolbox function PAL\_PFML\_BootstrapParametric created a set of simulated data based on the measured data and estimated  $\alpha$  and  $\beta$  for each simulation. Then the standard deviations (SD) on the parameters were determined. The number of bootstrap simulations was set to 400. For each psychometric curve, 99% confidence intervals (CI) for  $\alpha$  were estimated by multiplying the standard deviation with a factor of 1.96, where 1.96 is the 99% two sided fractile of the standard normal distribution. In addition a “confidence area” was determined giving a 99% confidence

that the fit will fall within. The outline of the area was built using the equation of the psychometric function with  $\alpha$  and  $\beta \pm 1.96$  SD. Four combinations of the parameters had to be applied to cover the whole area:  $\alpha - CI$  and  $\beta - CI$  for the lower half of the left border,  $\alpha - CI$  and  $\beta + CI$  for the upper half of the left border,  $\alpha + CI$  and  $\beta + CI$  for the lower half of the right boarder and  $\alpha + CI$  and  $\beta - CI$  for the upper half of the right border.

In order to determine whether the calculated psychometric function fits well to the measured data, a Goodness of Fit test was performed (Klein, 2000; Wichmann and Hill, 2001a). The  $\chi^2$ -statistic was calculated as given by

$$\chi^2 = \sum_i \frac{[p(data_i) - P_i]^2}{var(P_i)}, \quad (5)$$

where  $p(data_i)$  and  $P_i$  were the relative frequency of answers “acceleration” and the value of the psychometric function at stimulus level  $i$  respectively.  $Var(P_i)$  was the binomial variance defined by

$$var(P_i) = \frac{P_i(1 - P_i)}{N_i}, \quad (6)$$

where  $N_i$  is the number of trials at acceleration-level  $i$ .  $\chi^2$  is chi-square distributed depending on the degrees of freedom ( $df$ ). The degrees of freedom are given by the number of stimulus levels minus one. In the current study  $\chi^2$ -statistics on acceleration rates from  $-2.5 \text{ m/s}^2$  to  $2.5 \text{ m/s}^2$  were calculated, resulting in a  $df$  of 5. More extreme acceleration-rates were neglected, because the participants had answered correctly in the vast majority of cases. A significance level of 0.01 was chosen, which means that if the probability of getting the observed data is equal or less than the significance level, the supposed theoretical model (psychometric function) is not adequate to cover the observed data. Critical  $\chi^2$ -values could be easily read out using a  $\chi^2$ -distribution table. If the calculated  $\chi^2$ -value was smaller than the critical one, the curve is fitted well. The same procedure was also used to determine whether the narrowing psychometric curve significantly differed from the widening curve. Therefore,  $p(data_i)$  of the widening dataset and  $P_i$  of the narrowing function were used.

### 3 Results

Participants performed a yes-no-task, where they had to decide whether they had been accelerated or decelerated during a “flight” through a corridor which was either shaped straight, narrowing, or widening. Nearly all of the subjects noticed that the shape of the corridors changed among the different trials. Only subjects MG and DF weren’t conscious of the change. Nevertheless, knowledge about corridor geometry seemed not to have a direct effect on the results.

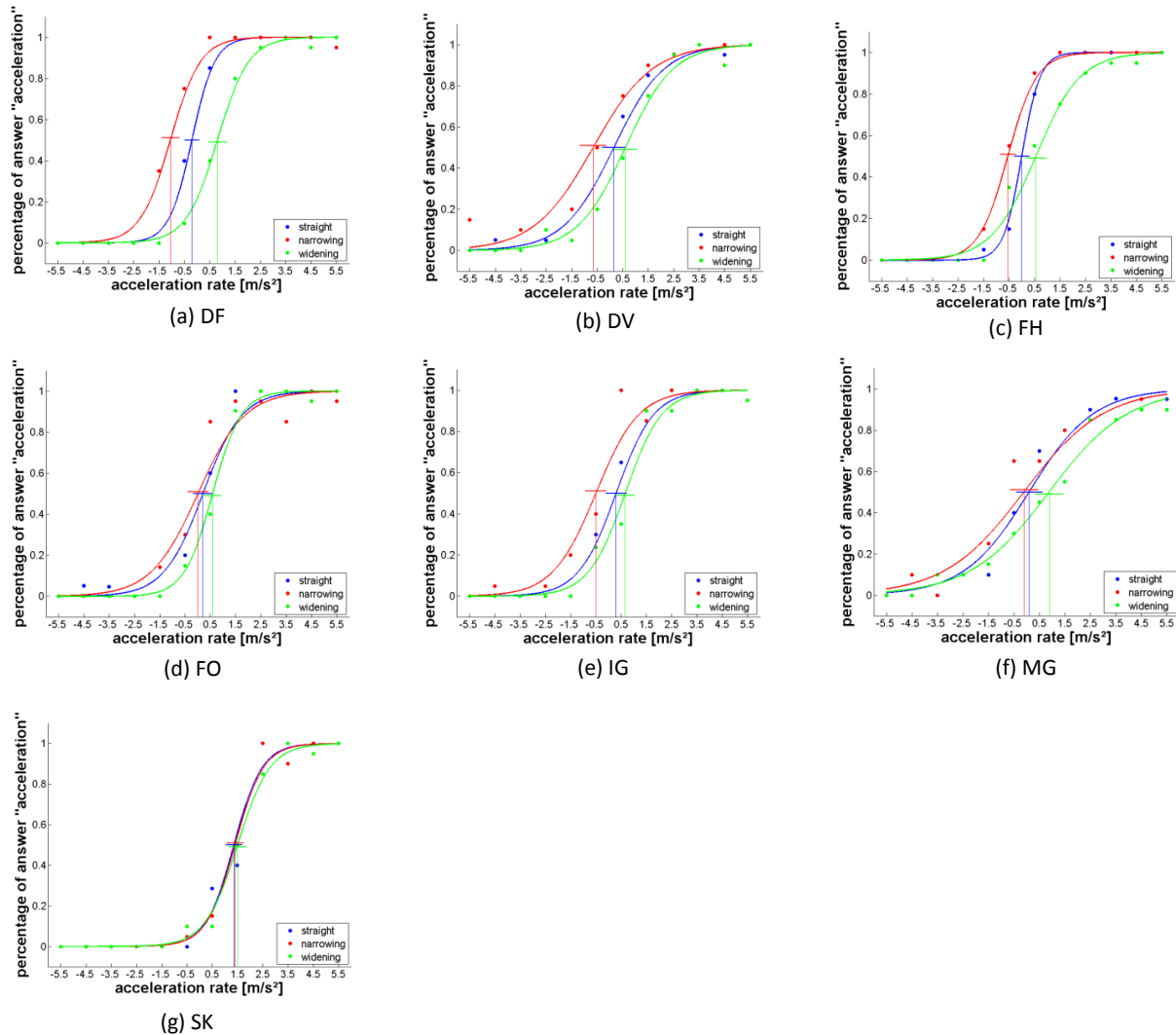


Figure 3.1. Psychometric functions for all seven subjects. Red: narrowing corridor; Blue: straight corridor; Green: widening corridor. Horizontal “error bars” show 99% confidence intervals. Vertical lines denote the point of subjective constancy (PSC). The threshold of the psychometric function for straight corridors lies around  $0 \text{ m/s}^2$ , whereas in the narrowing case thresholds are shifted towards deceleration and towards acceleration in the widening case (subject a-f).

Figure 3.1 shows fitted psychometric functions for all seven participants separately. The relative frequencies of answers “acceleration” were displayed against the different acceleration levels reaching from  $-5.5 \text{ m/s}^2$  to  $5.5 \text{ m/s}^2$ . For each stimulus level,  $20 \pm 1$  measurements were conducted. The threshold  $\alpha$  of the psychometric function indicated the perceived point of constant velocity (which will be referred to as either “point of subjective constancy “or PSC). In all participants, except for subject SK,

the psychometric functions were shifted towards deceleration in the narrowing case and towards acceleration in the widening case, which means that participants overestimated acceleration rates in the narrowing corridor and underestimated acceleration rates in the widening corridor. For the straight corridor, PSCs varied around  $0 \text{ m/s}^2$  and were shifted slightly towards acceleration. For subject SK the results were nearly the same for all three corridor conditions. Furthermore the psychometric curves had a strong bias ( $\sim 1.40 \text{ m/s}^2$ ) towards acceleration. Figure 3.2 shows psychometric functions for the three corridor conditions where the data of all participants have been merged. The fits are based on  $140 \pm 2$  measurements per stimulus level. As in the single subject plots, the curve was shifted towards deceleration ( $\alpha \pm \text{SD} = -0.20 \pm 0.08$ ) in the narrowing case and towards acceleration ( $\alpha \pm \text{SD} = 0.79 \pm 0.09$ ) in the widening case. The psychometric function for the straight corridor was located in the middle ( $\alpha \pm \text{SD} = 0.28 \pm 0.07$ ) of the two other curves. Points of subjective constancy (PCS) and slopes of the psychometric functions are listed in Table 3.1 and Table 3.2.

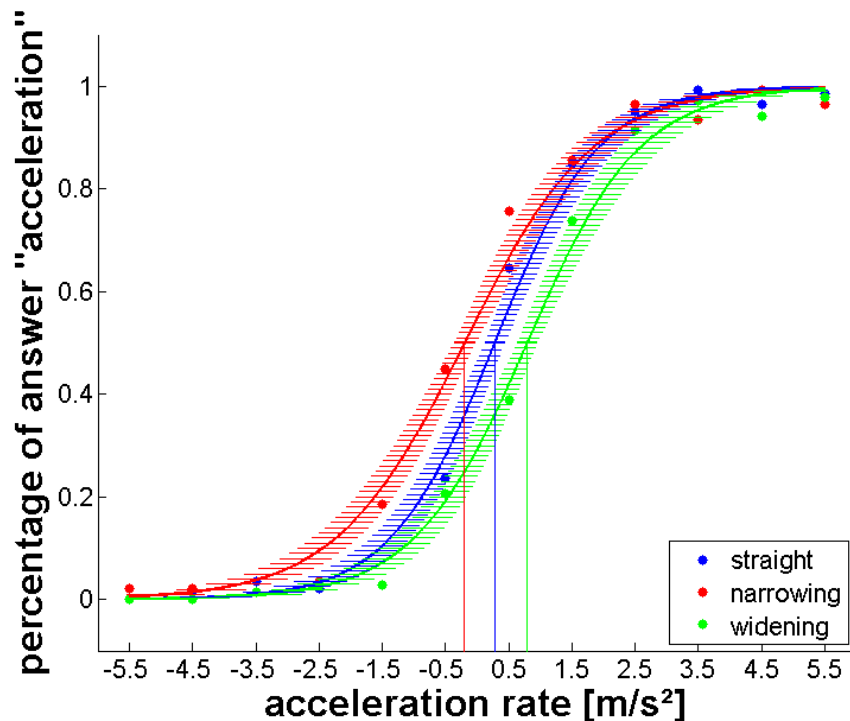


Figure 3.2. Combined data of all subjects and the resulting psychometric functions for all three corridor conditions. Red: narrowing corridor; Blue: straight corridor; Green: widening corridor. Horizontal "error bars" show 99% confidence intervals. The shaded faces depict 99 % confidence areas. Vertical lines denote the (mean) point of subjective constancy (PSC). The psychometric function of the narrowing corridor is shifted to the left, whereas the function for the widening corridor is shifted to the right. The curve for the straight corridor lies amidst them both.

Goodness of Fit tests of the psychometric functions were calculated on a range of  $-2.5 \text{ m/s}^2$  to  $2.5 \text{ m/s}^2$ . With a significance level of 0.01 and five degrees of freedom, the critical chi-square value was 15.086. Psychometric functions of subject DV, FH, FO, IG, MG and SK reliably fit the calculated data ( $\chi^2 < \chi^2_{crit}$ , see column 2 – 4 in Table 3.3 for goodness of fit). Only the fit for the straight corridor in subject DF significantly differed from the calculated data. ( $\chi^2 > \chi^2_{crit}$ ). The psychometric functions for the combined data of all subjects were fitted well for straight ( $14.68 < \chi^2_{crit}$ ) and widening ( $8.81 < \chi^2_{crit}$ )



corridors. The fit for the narrowing corridor differed significantly from the calculated data ( $15.80 > \chi^2_{crit}$ ). On the same theoretical basis, psychometric functions of the narrowing and the widening corridor were compared to test whether they differed significantly. In subject DF, DV, FH, FO and IG psychometric functions of the narrowing corridor and the widening corridor were significantly different from each other ( $\chi^2 > \chi^2_{crit}$ , see column 5 in Table 3.3 for comparisons). Comparisons in subject MG and SK didn't reach statistical significance. The fit of the combined data revealed a significant difference between the narrowing and widening corridor ( $125.03 > \chi^2_{crit}$ ).

Subject	Straight	Narrowing	Widening
DF	-0.20 ± 0.15	-1.05 ± 0.17	0.81 ± 0.18
DV	0.15 ± 0.23	-0.66 ± 0.26	0.60 ± 0.22
FH	0.21 ± 0.19	0.01 ± 0.21	0.59 ± 0.17
FO	0.00 ± 0.15	-0.55 ± 0.16	0.55 ± 0.20
IG	0.30 ± 0.20	-0.50 ± 0.21	0.66 ± 0.19
MG	0.10 ± 0.26	-0.10 ± 0.28	0.89 ± 0.28
SK	1.36 ± 0.16	1.40 ± 0.17	1.50 ± 0.18
<b>all subjects</b>	<b>0.28 ± 0.07</b>	<b>-0.20 ± 0.08</b>	<b>0.79 ± 0.09</b>

Table 3.1. **Thresholds** of the psychometric functions and standard deviations for all three corridor conditions in  $m/s^2$  ( $\alpha \pm SD$ ).

Subject	Straight	Narrowing	Widening
DF	2.20 ± 0.49	1.68 ± 0.31	1.61 ± 0.29
DV	1.01 ± 0.16	0.86 ± 0.12	1.06 ± 0.15
FH	1.29 ± 0.21	1.08 ± 0.14	1.78 ± 0.35
FO	2.78 ± 1.93	1.76 ± 0.34	1.15 ± 0.18
IG	1.34 ± 0.21	1.17 ± 0.18	1.38 ± 0.24
MG	0.79 ± 0.10	0.64 ± 0.08	0.65 ± 0.08
SK	1.79 ± 0.92	1.77 ± 0.36	1.55 ± 0.28
<b>all subjects</b>	<b>1.21 ± 0.07</b>	<b>0.98 ± 0.05</b>	<b>1.12 ± 0.06</b>

Table 3.2. **Slopes** of the psychometric functions and standard deviations for all three corridor conditions in  $1/(m/s^2)(\beta \pm SD)$ .

Subject	Straight	Narrowing	Widening	Narrowing compared to widening
DF	19,53	3,75	0,93	208,49
DV	4,58	2,57	4,06	27,00
FH	7,40	7,98	2,39	15,96
FO	2,27	1,59	4,45	101,34
IG	4,75	9,06	5,08	36,55
MG	3,42	5,33	1,58	9,61
SK	7,31	3,34	2,68	3,81
<b>all subjects</b>	<b>15,80</b>	<b>14,68</b>	<b>8,81</b>	<b>125,03</b>

Table 3.3. **Chi-Square Goodness of fit of all three corridor conditions and comparison** between the narrowing corridor and the widening corridor. Columns 2 -4 show the chi-square values for goodness of fit. The chi-square value in the fifth column is the result of testing the independency of the narrowing and the widening condition. With a significance level of 0.01 and five degrees of freedom the critical chi-square value is 15.086. A calculated chi-square value smaller than 15.086 means a good fit but also a not significant difference.

## 4 Discussion

### 4.1 Interpretation of the Results

The participants had to judge whether they had been accelerated or decelerated during a simulated flight through a corridor. The corridors were formed by two rows of solid colored blocks. The corridor appeared in three different conditions: straight, narrowing and widening. The stimuli were viewed through a stereoscope. Psychometric functions were fitted for each corridor condition depicting the relative frequency of answers “acceleration” as a function of the acceleration rate. Acceleration rate ranged between  $-5.5 \text{ m/s}^2$  and  $5.5 \text{ m/s}^2$  in steps of  $1 \text{ m/s}^2$ . The threshold of the psychometric functions is the perceived point of subjective constancy (PSC).

The findings of the present study were inconsistent with the initial prediction that participants are able to estimate their ego-acceleration, irrespective of the shape of the corridor. Figure 3.2 showed that the PSC of the narrowing function was shifted towards deceleration and the PSC of the widening function was shifted towards acceleration. Hence it can be concluded that the narrowing of the corridor leads to the illusion of increased ego-velocity, whereas the widening of the corridor leads to the illusion of decreased velocity. Despite detailed information about the three-dimensional structure of the scene being available, ego-velocity constancy could not be obtained. Although the psychometric functions significantly differed from each other, the results did not qualify for an evaluation of the shape-induced shifts in PSC. Therefore ego-velocity constancy could still have been involved to a limited extent. The question how the processing of optic flow interacts with the perception of object-observer distance remains to be answered.

### 4.2 Implications for Cue Integration

The perception of our world is characterized by a symphony of different sensory modalities, including motion, sight, sound, taste, touch and smell. All these modalities have to be integrated in the nervous system to form a stable, coherent and simultaneous picture of the world. The human benefits from cue integration in two ways: The first is to maximize the information which is delivered by the different sensory modalities (sensory combination). The second (sensory integration) is to disintegrate ambiguous sensory inputs, prioritizing the most reliable version (Ernst and Bühlhoff, 2004). For example, when we sit in a stationary train looking out of the window at another train just beginning to move, we will immediately have the illusion of self-motion until our vestibular system tells us better.

Festl et al. (2012) showed that optic flow has a strong influence on the estimation of ego-acceleration, proposing a matched filter mechanism for the processing of optic flow. The subsequent studies of Becker (2013) gave evidence that not only optic flow, but also stereoscopic depth influences computations for ego-acceleration. In fact, it can be argued that some integration between stereopsis and optic flow processing must have occurred. Therefore it seems plausible to assume that multiple cues are combined to estimate ego-acceleration in a realistic environment. Due to a lack of comparability, one can only speculate which visual cues entered the computations of ego-acceleration in the current experiment. Although participants still confuse actual ego-acceleration with scene geometry, velocity constancy could have, if not completely, been at least partially obtained. For example, when the corridor narrows down, the optic flow becomes bigger, but the distance between the observer and the blocks is reduced. If

complete velocity constancy could be obtained, the observer would be able to compensate the increase in optic flow with an estimate of the decrease in distance. The increasing angular size of the blocks, stereoscopic disparity and motion parallax (structure from motion) provided information that could have been used to measure differences in the distance between the observer and the borders of the corridor. However, most of the participants reported, that they were aware of the different corridor shapes. Nevertheless, this knowledge did not suffice to disentangle corridor shape and egomotion in the ego-acceleration estimation task.

### 4.3 Comparability to previous findings

The present study tried to replicate the experimental design of its precursors as far as possible. As in Festl et al. (2012) and Becker (2013) twelve different accelerations levels were chosen, ranging between  $-5.5 \text{ m/s}^2$  and  $5.5 \text{ m/s}^2$  in steps of  $1 \text{ m/s}^2$ . Furthermore the duration of the motion sequences (3 seconds) and the overall travel distance (30 meters) had been adopted. In the present study and the study of Becker (2013), the stimuli subtended approximately  $41^\circ$  horizontal visual angle and  $24^\circ$  vertical visual angle. The field of view in the setup of Festl et al. (2012) subtended a visual angle of  $23^\circ$ , both in horizontal and vertical direction. Despite the similarities, the stimuli fundamentally differed in their characteristics. First of all, the geometry of the corridor was no longer determined by a fuzzy cloud of random dots (Figure 4.1), but by an array of distinct three-dimensional objects (Figure 2.2). Therefore scene segmentation and object recognition opened up a new visual quality for the observer. Another point is that the observer no longer traveled in the middle of a tube, but rather moved on a street like a car driver. In contrast to the random dot stimulus, the only optic flow generated, emerges from the left and right side of the corridor. Furthermore the apical angle of the tubular corridors was  $2^\circ$ , whereas the apical angle was only  $1^\circ$  in the block corridor.

In the study of Festl (2012) the threshold of the narrowing tunnel was around  $-2.5 \text{ m/s}^2$  and for the widening tunnel around  $3.3 \text{ m/s}^2$ . In the study of Becker (2013) the shifts in the psychometric functions were reduced considerably to  $-0.8 \text{ m/s}^2$  for the narrowing tunnel and  $2.2 \text{ m/s}^2$  for the widening tunnel. In the current study, the thresholds were  $-0.2 \text{ m/s}^2$  for the narrowing corridor and  $0.8 \text{ m/s}^2$  for the widening corridor. Due to general differences in the stimulus, the present study cannot be directly compared with the prior ones.

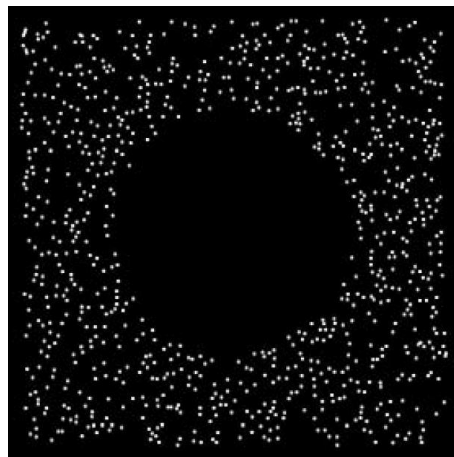


Figure 4.1 Dynamic optic flow pattern as used in Festl et al. (2012) and Becker (2013).

#### **4.4 Future prospects**

The next step will be to conduct a control experiment with shrinking blocks for the narrowing corridor and with increasing blocks for the widening corridor, to test for the effect of object size. Prior knowledge about the object and top-down processing could also play a role in ego-acceleration estimation and should be investigated in the future. As a follow up, another random dot study will be conducted, where participants have to dynamically adjust their ego-velocity with a joystick. The stimulus consists of a tubular corridor which periodically contracts and expands causing the illusion of acceleration or deceleration. In the task the participants are then asked to keep their speed at a constant level.

To understand the perception of ego-acceleration in a natural environment, particular attention should be paid to how optical flow processing interacts with the processing of depth. And therefore it should be quantified how the different depth cues, such as stereopsis, motion parallax, texture, shading and perspective size enter the computation of ego-acceleration.

## Bibliography

- BECKER, T. 2013. Detection of linear ego-acceleration from optic flow in stereoscopy. Msc Thesis, Graduate School of Neural & Behavioral Sciences, Eberhardt Karls Universität Tübingen.
- BÜLTHOFF, H. H. and H. A. MALLOT. 1988. Integration of Depth Modules: Stereo and Shading. *JOSA A*, 5:1749-1758.
- CHARLES, W. 1838. On Binocular Vision: And on the Stereoscope, an Instrument for Illustrating Its Phenomena. *Report to the British Association for the Advancement of Science* Pt:16-17.
- DISTLER, H. K., K. R. GEGENFURTNER, H. VAN VEEN and M. J. HAWKEN. 2000. Velocity Constancy in a Virtual Reality Environment. *Perception, London*, 29:1423-1436.
- ERNST, M. O. and H. H. BÜLTHOFF. 2004. Merging the Senses into a Robust Percept. *Trends in Cognitive Sciences*, 8:162-169.
- FESTL, F., F. RECKTENWALD, C. YUAN and H. A. MALLOT. 2012. Detection of Linear Ego-Acceleration from Optic Flow. *Journal of Vision*, 12.
- FRENZ, H. and M. LAPPE. 2005. Absolute Travel Distance from Optic Flow. *Vision Research*, 45:1679-1692.
- GIBSON, J. J. 1950. *The Perception of the Visual World*. Boston: Houghton Mifflin.
- GIBSON, J. J. 1958. Visually Controlled Locomotion and Visual Orientation in Animals. *British Journal of Psychology*, 49:182-194.
- HANNIG, M. 2012. Entwicklung und Validierung eines spiegelstereoskopischen Virtual-Reality Aufbaus. Diplomarbeit, Bioinformatics, Eberhardt Karls Universität Tübingen.
- KAISER, M. K. and H. HECHT. 1995. Time-to-Passage Judgments in Nonconstant Optical Flow Fields. *Perception & Psychophysics*, 57:817-825.
- KLEIN, S. A. 2001. Measuring, Estimating, and Understanding the Psychometric Function: A Commentary. *Perception & Psychophysics*, 63:1421-1455.
- KOLLIN, J. and A. HOLLANDER. Re-Engineering the Wheatstone Stereoscope. *SPIE Newsroom*. doi: 10.1117/2.1200702.0673.
- LEE, D. N. and E. ARONSON. 1974. Visual Proprioceptive Control of Standing in Human Infants. *Perception & Psychophysics*, 15:529-532.
- LONGUET-HIGGINS, H. C. and K. PRAZDNY. 1980. The Interpretation of a Moving Retinal Image. *Proceedings of the Royal Society of London. Series B. Biological Sciences*, 208:385-397.
- WARREN, W. H., B. A. KAY, W. D. ZOSH, A. P. DUCHON and S. SAHUC. 2001. Optic Flow Is Used to Control Human Walking. *Nature Neuroscience*, 4:213-216.
- WHEATSTONE, C. 1852. The Bakerian Lecture--Contributions to the Physiology of Vision.--Part the Second. On Some Remarkable, and Hitherto Unobserved, Phenomena of Binocular Vision (Continued). *Philosophical Transactions of the Royal Society of London*, 142:1-17.
- WICHMANN, F. A. and N. J. HILL. 2001. The Psychometric Function: I. Fitting, Sampling, and Goodness of Fit. *Perception & Psychophysics*, 63:1293-1313.

## **Acknowledgements**

First of all I am grateful that Prof. Dr. Hanspeter Mallot allowed me to write my Bachelor-Thesis in the cognitive neuroscience lab. I would like to thank him for numerous valuable inputs, inspiration and encouragement. I would also like to thank Dr. Gregor Hardiess and Dr. Hansjürgen Dahmen for interesting discussions during the optic flow meetings and for their cordial kindness. Thanks also to Marc Halfmann who helped me with the technical aspects of my work. Furthermore I am thankful to all members of the cognitive neuroscience lab and my fellow students for having had this experience in such a humorous, friendly and enriching atmosphere. Finally, thanks go to my family who always supported me in various ways during my studies.